High-speed high spatial resolution magneto-optic Kerr effect polarimeter/microscope for studies of ultrathin magnetic structures

Marcus Heidkamp and J. L. Erskine
Physics Department, The University of Texas at Austin, Austin, Texas 78712

(Received 23 November 1999; accepted for publication 21 April 2000)

A magneto-optic Kerr effect polarimeter designed to study the dynamics of magnetization reversal in ultrathin films, multilayer films, and microstructures is described. The polarimeter is integrated into a long focal-length charge coupled device (CCD) camera based Kerr microscope that permits viewing domain structures and facilitates positioning of the focused polarimeter beam on microstructures in ultrahigh vacuum. Diffraction-limited spatial resolution, based on the *f*-number of the respective objective lenses, is achieved by the microscope (~ 1 μm) and polarimeter (~ 5 μm). The polarimeter is capable of measuring continuous wave or repetitive transient ultrathin film magnetic response at sampling rates of 40 million samples/s (MS/s) over a micron-scale region defined by the illuminating spot. Hysteresis loops generated by ultrathin (monolayer) films and microstructures can be measured at high signal-to-noise ratio over a nine-decade range of drive frequencies. © *2000 American Institute of Physics.* [S0034-6748(00)00708-5]

I. INTRODUCTION

A broad variety of magnetic sensitive polarimeters and microscopes, based on the magneto-optic Kerr effect, have been developed to study magnetic phenomena in thin magnetic films.[1–14] Recent adaptations have combined Kerr microscopes[3–6] based on charge coupled device (CCD) cameras with laser-based polarimeters[7–10] having incident beams focused to the diffraction limit. These instruments achieve the versatility and high spatial resolution required to probe magnetic properties of microstructures. Pump–probe[11,12] and related stroboscopic[13] techniques based on pulsed-laser excitation have also been used in magneto-optical studies of magnetic response at high spatial and temporal resolution. The spatial resolution of Kerr microscopes and polarimeters has been increased beyond the diffraction limit by utilizing near-field techniques,[14] and microelectronic processing technology[10] has been used to create submicron magnetic structures that can also be studied by magneto-optical techniques. In these cases, the lower limit on the size of structures that can be effectively studied is governed only by the strength of magneto-optic response and the sensitivity of the polarimeter. Clearly, the magneto-optic Kerr effect provides the basis for a broad range of versatile probes of magnetic phenomena.

The present paper describes a Kerr microscope high-speed magneto-optic polarimeter combination that has been developed to study dynamical effects in ultrathin film magnetic structures. One goal in setting up the new instrument was to add several decades to the frequency range over which magnetic hysteresis and energy loss scaling[15,16] of ultrathin film structures could be probed. A second goal was to achieve the high spatial resolution and high sensitivity required to enable direct measurements of domain wall velocities in micron-scale ultrathin film structures. Both goals have been achieved by our new instrument. The polarimeter is currently capable of measuring hysteresis loops of ultrathin films over a frequency range from below 10^{-3} Hz to above 1 MHz (at 2 MHz the loop is defined by 20 points) or sampling a repetitive magnetic transient at a rate of 40 MS/s. Our planned experimental studies of domain wall motion and energy loss scaling vs selected control parameters such as temperature, applied drive field strength H (and dH/dt), and materials parameters including microstructure size, shape, and composition should lead to more precise understanding of the atomic level phenomena that underlie magnetic switching in thin film structures.

II. KERR MICROSCOPE/POLARIMETER

The new Kerr microscope/polarimeter has been designed to adapt to an existing film growth and characterization instrument.[1] In order to maintain a configuration compatible with magnetic response measurements at low temperature and in an ultrahigh vacuum environment, both the polarimeter and microscope designs employ long focal-length optics. Figure 1 displays a schematic diagram of the Kerr microscope/polarimeter combination. The microscope and polarimeter are mounted on an optical table that is designed to clamp rigidly to the ultrahigh vacuum chamber. A rigid connection is required because the polarimeter microscope objective is mounted inside the vacuum chamber on the same flange assembly that mounts the Kerr microscope viewport. The microscope is mounted on a micrometer driven *x-y* table that permits focusing and positioning of its field of view. The sample is mounted on a precision *xyz* rotation+tilt manipulator that provides access to thin film growth [molecular-beam epitaxy (MBE) with masks] and characterization [low-energy electron diffraction (LEED) and Auger electron spectroscopy].[1] The sample is mechanically stabilized at the common focal point of the magneto-optic Kerr effect polarimeter and microscope by a precision *x-y* device similar to a transmission electron microscope (TEM) specimen stage. Mechanical stability and reduction or elimination of vibra-

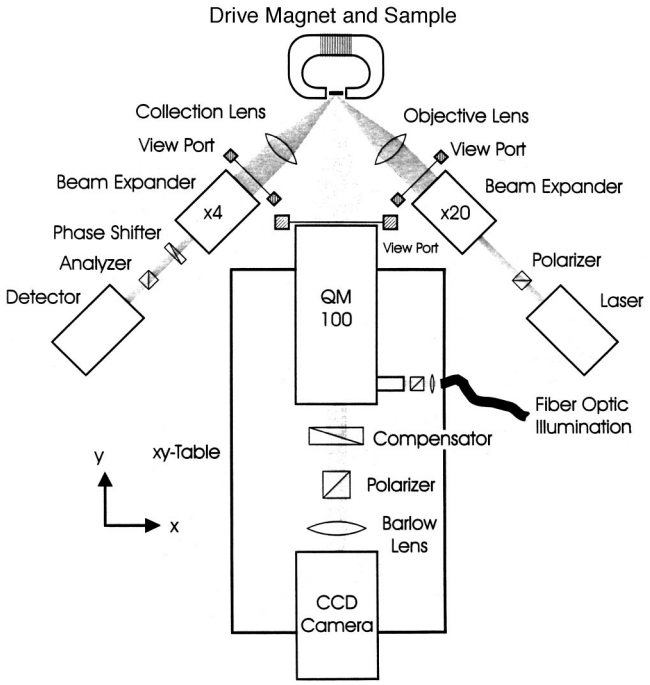

FIG. 1. Block diagram of Kerr microscope/polarimeter describing the optical configuration and principal optical components. The polarimeter is shown in a single beam configuration (no reference channel) to simplify the drawing. Text contains additional details covering components.

tional resonances are important factors in obtaining high sensitivity and high spatial resolution in a Kerr microscope or Kerr polarimeter.

A few comments are in order regarding factors that must be addressed when hysteresis loop measurements are carried out over a broad range of drive frequencies. At very low drive frequencies (0.001 Hz), loop averaging is not feasible, but if probing Barkhausen noise is not the objective, sampling the magnetization, M, at random values of H can reduce the undesirable effects of mechanical and electronic drift, laser fluctuations (both intensity and spatial), and light scattering by dust particles. Significant problems associated with mechanical resonances can be encountered from subaudio frequencies through several kHz. Most of the problems involve the sample mount being driven by the magnet. Loop averaging that occurs at higher frequencies reduces the undesirable effects of mechanical resonances, but it is wise to eliminate magnetic materials on the sample manipulator, and reduce eddy current forces by restricting the use of metallic parts near the magnet gap to a minimum.

Good electrical shielding and grounding are required to keep magnet drive signals from the sensitive signal channels. While the highly nonlinear hysteresis signals are easily separated from sinusoidal or linear ramp magnet drive waveforms, sensitivity of the polarimeter can be reduced due to limited dynamic range of detection instruments if a high level noise signal is superimposed on the magnetic signal.

The dynamic range of the polarimeter described in this paper is governed by the 12-bit A/D converter used to measure the signal. Optimum contrast in a polarimeter[1] is governed by the extinction ratio of the optical system and is obtained by setting the analyzing prism a few degrees away from the extinction condition. The offset is also required to achieve the linear relationship between changes in measured intensity and sample magnetization necessary to obtain a hysteresis loop. A typical extinction ratio for the polarimeter shown in Fig. 1 including effects resulting from viewports, beam expanders, lenses, etc., is $\varepsilon \sim 5\times 10^{-4}$, which results in an optimum polarizer offset of $\theta \sim 0.023$ rad (1.3°). The Kerr microscope achieves a similar extinction ratio and the same principle governs the settings required to optimize the magnetic contrast. A dual beam detection system (described later in Fig. 3) is used to reduce undesirable effects of laser intensity drift and fluctuation and to take full advantage of the 12-bit dynamic range in measuring the magnetic contrast. By subtracting the direct current (dc) voltage (produced by the polarizer offset) from the signal channel using a differential amplifier prior to the A/D conversion, the amplitude of the signal plus noise can be matched to a full-scale sensitivity range of the A/D card.

A. Kerr microscope

The Kerr microscope in Fig. 1 is based on a Questar QM-100 long focal-length microscope coupled to a Princeton Research Pentamax CCD camera. A standard 150 W tungsten halogen fiber-optic laboratory source and lens provides uniform on-axis illumination through a prism in the microscope. Glan-Taylor prisms are used to polarize and analyze the light, and a 25 mm Babinet-Soleil compensator is used to optimize the contrast. The microscope optics achieve an extinction ratio of $\sim 5\times 10^{-5}$, which is comparable to that obtained by the polarimeter. Similar Kerr microscopes have been reported,[3–6] therefore the description of this subassembly of the instrument is brief. The QM-100 in our configuration is positioned at the optimum working distance of 10 cm and yields a nominal magnification of 10× that images a 0.5 mm field of view at the sample onto the CCD detector (Kodak KAF-1400) which has 1317 H×1035 V pixels and physical dimensions of 8.98 ×7.04 mm^2. Barlow lenses (×2 or ×3) placed between the microscope and camera can be used to expand the image (increase the magnification).

Figure 2 displays the image of a microscope test pattern consisting of 2.5-μm-wide chromium strips on a glass substrate obtained using polarized white light illumination, and ×10 magnification. The image was obtained through a standard $4\frac{1}{2}$-in.-o.d. conflat flange viewport (the cone of light from the sample intercepts approximately 60% of the viewport area). The image is unprocessed. The camera is capable of capturing a 1317×1035 pixel 12-bit dynamic range image every 200 ms. It is clear that the QM-100/Pentamax combination easily resolves 2.5 μm features with center-to-center separation of 5 μm. The ultimate resolving power of the QM-100 is stated to be 1.1 μm at a focal distance of 10 cm. Based on the results presented in Fig. 2 it is clear that this limit is approached, if not achieved. Slightly sharper test pattern images (with a smaller field of view) are obtained using a blue filter and a ×2 or ×3 Barlow lens to increase the pixel density of the image. Software provided with the camera by Princeton Instruments permits the image manipulation and processing required to obtain Kerr microscope do-

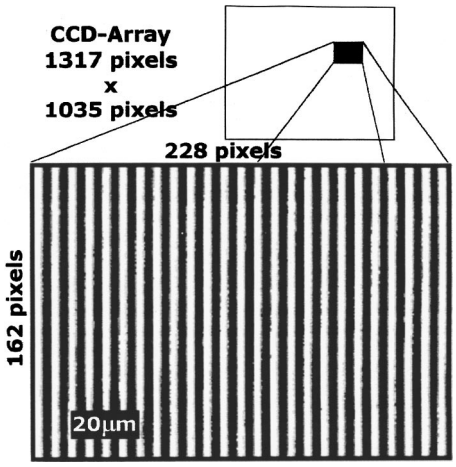

FIG. 2. Polarized light test pattern image obtained through a standard ultra-high vacuum viewport using the QM-100 microscope and CCD camera. Test target consists of chromium strips on glass with 5 μm spacing. The magnification was 10×(no Barlow lenz) yielding a ~1 mm diameter field of view. The CCD camera pixel density is indicated in the blow-up and a 20 μm ruler is inserted to indicate scale. Resolution is estimated to be about 1 μm.

main images. High sensitivity required to obtain good quality domain images from the low-contrast Kerr effect is obtained by frame integration and most of the morphological (non-magnetic features in the microscope images) can be removed by subtracting frame-averaged images taken when the magnetic film is saturated (no magnetic contrast).

The microscope/polarimeter configuration permits viewing both polar Kerr effect images (using illumination through the microscope) and longitudinal Kerr effect images (using illumination through the polarimeter). In the latter case, the sample must be rotated 22.5°. The non-normal viewing configuration results in a reduction of the field of view over which high-resolution images can be obtained due to the shallow depth of focus. In principle, part of the field can be recovered by tilting the image plane.[17]

B. High-speed high spatial resolution polarimeter

Figure 3 displays a more detailed schematic diagram of the high-speed high spatial resolution polarimeter including principal optical elements and electronic components. High spatial resolution is achieved while maintaining a reasonable working volume surrounding the sample by using large aperture lenses with suitable focal lengths. Our polarimeter currently utilizes lenses having 1 in. clear apertures and 3 in. focal lengths. The focal length provides adequate space for in-vacuum magnets required to drive the magnetic films and the 1 in. aperture is compatible with the relatively strain-free region of standard $2\frac{3}{4}$ in. conflat flange viewports. The lens parameters yield a numerical aperture of 1/6 (f number of 3), which produces a diffraction-limited spot of about 4.5 μm diameter for $\lambda = 6328$ Å. Scattered light from the focused polarimeter beam is conveniently imaged by the microscope, providing means of focusing and positioning the light spot in the field of view. A 20× beam expander is used on the source arm to increase the (nominal 1 mm diameter) laser beam to the 20 mm diameter required to take advantage of

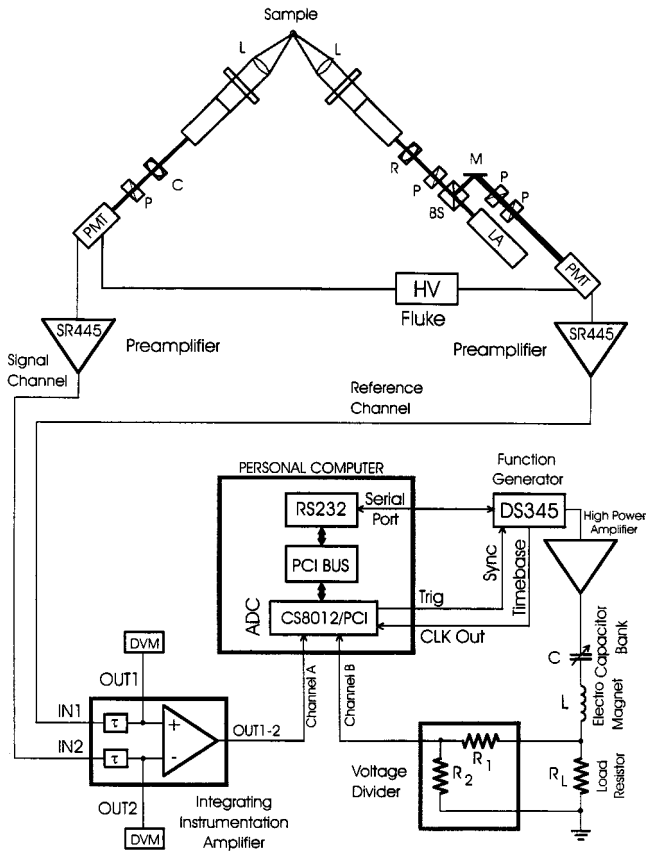

FIG. 3. Block diagram of Kerr effect polarimeter (dual beam configuration) showing principal electronic components. Text contains additional details.

the polarimeter objective lens. A 4× beam expander is used in conjunction with a second objective lens to recover a small diameter parallel beam.

The data acquisition and processing strategy for the Kerr effect polarimeter was developed around a CompuScope 8012/PCI card manufactured by GaGe Applied Sciences, Inc. This card incorporates a 12-bit analog-to-digital converter with fast on-board memory. Sampling rates can be varied from 1 Hz to 80 MHz (40 MHz dual channel mode) in steps of 1, 2, 5, 10, 20 ..., and the on-board memory can store 10^6 12-bit samples. The system can be upgraded to permit 100 MHz dual channel operation by using two GaGe 8012 A/PCI units in a master/slave configuration. In order to permit M-H measurements at high temporal resolutions (up to 25 ns/sample in dual channel mode) and also be able to trace loops at low sweep rates (1 mHz), an integrating differential amplifier is used between the detector/preamps and the scope card. A differential amplifier is required to utilize the split beam configuration shown in the figure, and an integrating stage with variable time constants is required to integrate the detected intensity between A/D sampling, especially at low frequencies.

Photomultiplier tubes are used for light detection (Hamamatsu R374) when high temporal resolution is required. This tube has a 28 mm diameter multialkali cathode and offers relatively high gain (5×10^6) and fast (15 ns) response. The quantum efficiency of photomultiplier tubes, especially in the red part of the visible spectrum ($\lambda = 6328$ Å), is poor compared with silicon detectors; how-

ever, the large detector area (which reduces microphonic effects), high noise-free gain, and fast response of a photomultiplier tube render it a good choice for high sampling rate measurements. Since the signal channel and reference channel have independent polarimeters, both tubes can be operated from the same high voltage power supply. This reduces differential changes in tube gain resulting from voltage drifts.

Stanford Research Systems (SR-445) DC-coupled 300-MHz bandwidth amplifiers (with 50 Ω input impedance selected) are used to increase the photomultiplier tube output voltage prior to subtracting the DC component from the signal channel. The detected light level in the signal channel arm of the polarimeter is governed by the laser intensity (in this case a 1 mW laser) and the setting of the polarimeter optical elements that yield maximum contrast.[1] A photomultiplier tube provides high gain at an excellent noise figure, therefore the tube gains are maximized by choosing an anode current of ~80 μA (the maximum recommended anode current is 100 μA) under conditions of optimum contrast. Three stages of ×5 gain in the SR-445 amplifiers yield signal and reference channel voltages of 0.5 V that are input to the integrating differential amplifier.

The integrating differential amplifier was constructed using video operational amplifiers (LM6172I) that offer unity gain bandwidth of 100 MHz. The overall gain of the differential amplifier is about ×5, and the −3 dB bandwidth for the minimum time constant integration setting is above 15 MHz. This bandwidth is adequate for the maximum A/D sampling rate available from the GaGe scope card operating in dual channel mode (40 M samples/s). The rise time for a single-stage low-pass filter having a −3 dB bandwidth of B is $\tau = 0.35/B$. Based on this criterion, the rise time of the electronic circuitry which is limited by the integrating amplifier response is just over 20 ns, which is essentially equal to the maximum sampling rate of the A/D card used in the polarimeter. Extensive continuous wave (cw) and pulse measurements[18] of the amplifier response established that the cutoff frequencies were well-behaved and accurately governed by the time constant settings, and that the common mode rejection ratio was good: it was about 75 dB at low frequencies (<100 Hz), and decreased monotonically to about 55 dB at 30 MHz.

At low drive frequencies (below 10 Hz), the signal-to-noise ratio departs significantly from the theoretically predicted value when the photomultiplier PM tube wide-band amplifiers are used (described later in Sec. IV). Substituting silicon detectors with integrated preamplifiers (New Focus Model 2301) yields much better performance at low frequency. These detectors are large area (~1 cm^2) detectors with integrated amplifiers that provide 10^6 V/A gain and a 90 kHz bandwidth. They can be directly substituted for the PM tube/300 MHz amplifier combination for better performance at low sampling frequencies.

C. Data acquisition software

Efficient and accurate measurements of magnetic hysteresis loops and switching transients based on A/D conversion of the wide-bandwidth analog signals produced by the polarimeter required development of data acquisition software. Even under optimum conditions (in which the signal-to-noise ratio of the Kerr effect signal is limited by statistical noise), several minutes of signal averaging are often required to generate a high-resolution hysteresis loop (i.e., 1000 points with S/N>50) for monolayer thickness films. Excellent S/N ratio loops for thick (~100 Å) films can be obtained in a few seconds. Digitized waveform averaging using 12-bit resolution at effective sampling rates of 80 MS/s creates a huge data stream in a short time (a 2 min experiment would generate 18 GB of raw data). For most of the sampling rates used in typical magneto-optical experiments, a fast PC processor (200 MHz) is able to signal average the data stream in real time during data acquisition. Therefore, the data acquisition strategy adopted for operating the high-speed polarimeter is based on a burst mode in which the scope card buffer accumulates a data stream while the PC processes (signal averages) the prior contents of the buffer. Transfer of the buffer memory data file to the PC RAM through the PCI bus is a fast process, and does not contribute appreciably to measurement dead time (at least at low sampling frequencies).

In a typical loop averaging sequence, the scope card RAM stores a data stream file consisting of many cycles of the $M(t)$ and $H(t)$ waveforms, and a large number of scope card RAM files are transferred to the PC for signal averaging. In order to ensure that each cycle of the RAM file waveform is properly added when performing the averaging, a strategy is required that locks the phase of the RAM waveforms. The triggering feature of the scope card permits beginning the digitizing process at a specified point in the waveform. However, since the scope card and signal generator have independent crystal oscillator time bases, there is no guarantee that each digitized RAM file wave stream will remain properly synchronized for signal averaging.

The solution to this problem is to phase lock the function generator time base to the master clock of the analog-to-digital converter (ADC) card. The ADC card and the signal generator both use 40 MHz master clocks, and the signal generator has the capability to phase lock with an external signal. In addition, it produces a sync output pulse that can be used to precisely trigger the point at which the ADC begins to digitize a data stream.

We note that frequency-dependent phase shifts occur in both the analog detection electronics and in the drive magnet circuit. The absolute phase shift through the system is required to obtain an accurate value of H_c^* from a hysteresis loop measurement at any specified drive frequency and amplitude. We perform such calibrations[16] by placing a glass prism at the sample position and measuring the Faraday effect. Other strategies based on fast electro-optic modulation systems are also expected to yield accurate phase shift and time delay calibrations. Drifts in the phase shift during the time required to signal average a hysteresis loop can also affect the temporal resolution. However, for a 1000 point loop, as long as the phase drift is less than 0.1% of 2π, the effect is not detected by the measurement.

Once the ADC and signal generator master clocks are phase locked and the ADC data stream bursts are synchro-

nized with the drive signal by a timing pulse from the generator, the only remaining task is to select the drive frequency and the sampling frequency such that one drive frequency cycle has an integral number of sample points (the number of points that will define the hysteresis loop or repetitive magnetic transient). The relationship is simply $f_d = f_s/p_s$, where f_d=drive frequency, f_s=sampling frequency, and p_s=the number of sample points per cycle. Since the ADC sample frequency f_s is restricted to (1, 2, 5, 10 ... 10 M, 20 M, 40 M) Hz, there are constraints on f_s and p_s. In our software, the user specifies f_d and p_s, and an algorithm determines the closest allowable values of these parameters that are compatible with the constraints on the ADC sampling rate.

The computer software that drives the scope card A /D and the signal generator was implemented using Microsoft Visual C++, and operates under Microsoft's Windows95 operating system. The data acquisition program displays the signal-averaged (full single period) waveforms $M(t)$ and $H(t)$, as well as the M-H loop during data acquisition (Fig. 4). A menu-driven interface permits convenient selection of measurement parameters and the export of signal-averaged data as ASCII files. Plotting, statistical analysis, and curve fitting of the data are carried out using commercial software such as MATHEMATICA and IGOR.

III. PERFORMANCE EVALUATION OF POLARIMETER

Performance evaluations of the polarimeter were carried out using a Faraday cell and also using a thin magnetic film. A Faraday cell consisting of a glass rod inside a solenoid is a useful device for calibrating and testing a polarimeter. The polarization rotation from the Faraday effect is a linear (and instantaneous) function of the field produced by the solenoid. The sensitivity of the polarimeter was tested by measurements of the Faraday rotation at low solenoid currents, and undesirable background signals coupled into the detection electronics were determined by running the Faraday cell solenoid at high currents with the glass rod removed. Similar experiments using a glass prism (to produce Faraday rotations) or a nonmagnetic mirror placed between the magnet pole caps have also been used to measure phase shifts between the magnet current and magnetic fields and to test polarimeter response.[16]

A permalloy film was chosen for initial hysteresis loop measurements. A low-coercivity film was required because the drive magnet (in this case) consisted of a pair of coils (20 turns on 8 mm diam glass rods) with modified Helmholtz geometry (separation equal to coil diameter rather than radius). The coils produced about 5 G/amp at 8 mm separation. Three power amplifiers were available to drive the coils, a Kepco bipolar operational power supply (20 amp/15 volt) a 300 W McIntosh audio amplifier, and an ENI 240L rf amplifier. The Kepco provided 15 amps into a 1 Ω load (R_L in Fig. 3) from DC through about 1 kHz the Mclntosh (vacuum tube/transformer model) provided over 17 amps into 1 Ω from 15 Hz through 50 kHz, and several amps at 100 kHz. The ENI amplifier (50 Ω output impedance) was coupled to the 1 Ω load and coil through a ferrite-core impedance matching transformer. This combination provided (with suitable capacitors to cancel the coil inductive reactance) 10 amps to the coil over a frequency range from 20 kHz through 10 MHz. Our initial tests have covered drive frequencies from 10^{-3} Hz through 2 MHz. At 2 MHz, a loop is defined by only 20 points by our existing A/D card. A planned upgrade, described later, will permit dual channel operation at 100 MHz (20 points per loop at 5 MHz drive frequency).

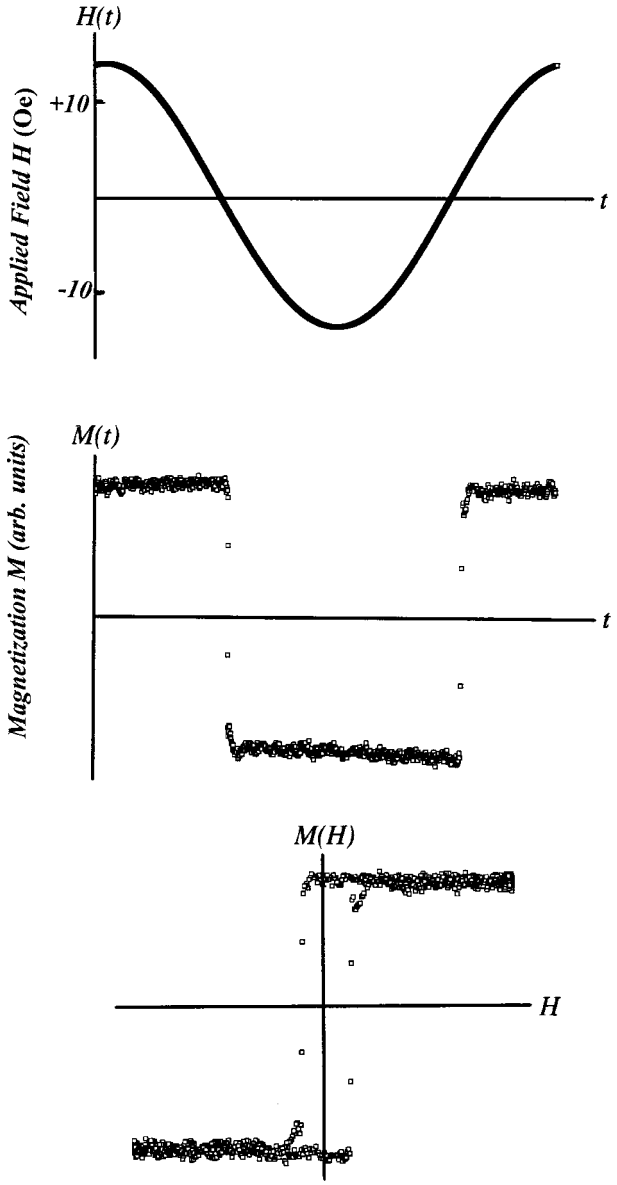

FIG. 4. Typical averaged waveforms $H(t)$ (sine wave drive current) and $M(t)$ (Kerr signal from polarimeter) plus the hysteresis loop $M(H)$ derived from $M(t)$ and $H(t)$. Parameters: drive frequency 2010.5 Hz, analog time constant $RC=10^{-7}$ s, number of points $N=995$, A/D sample rate 2.0 MS/s (time resolution 500 ns between samples). In this case, the S/N ratio is approximately 25.

The $Ni_{89}Fe_{19}$ permalloy film was grown on a Si(001) substrate that had a 100 nm SiO_2 layer on it.[19] The 300 nm magnetic layer was sandwiched between 5 nm Ta layers to stabilize it against oxidation. The film was grown in the presence of an in-plane magnetic field which established an easy ($H_s \sim 2$ Oe) and a hard ($H_s \sim 8$ Oe) in-plane axis 90° from the easy axis.

Figure 4 displays a typical hysteresis loop measured by the polarimeter. The applied magnetic field parameters for this loop were $H=\pm 14$ Oe at $f=2010.5$ Hz. The permalloy film was oriented with its easy axis parallel to the applied field. The dynamic coercivity $H_c^*=3.5$ Oe is only slightly higher than the ''dc'' coercivity measured by a superconducting quantum interference device (SQUID) magnetometer. A slight (0.40 Oe) offset is apparent from the hysteresis loop; this offset is a result of the earth's magnetic field. Additional hysteresis loop measurements of the same film using drive frequencies from $10^{-3}-10^6$ Hz yielded loops similar to the one displayed in Fig. 4. H_c^* increased with frequency as expected,[15,16] and at high drive frequencies and the fastest sampling rates (25 ns sample) the film transient response was defined by more points, indicating the finite switching speed of the film. Accurate transient response calibrations of the polarimeter using an electro-optic modulator (Con Optics Model 350–160 with a 25D driver that delivers an 8 ns rise time) have shown that the PM tube response and analog electronics are fast enough to take full advantage of the highest (20 ns) A/D sampling rate of our scope card.

The sensitivity and noise characteristics of the polarimeter were determined using a Faraday cell polarization modulator. The Faraday cell consisted of a 5-cm-long glass rod in a solenoid. The glass rod was mechanically isolated from the coil and could be removed to test for spurious signals resulting from inductive or capacitive coupling. The rotation produced by the Faraday cell was calibrated by measuring the mechanical rotation of the analyzing prism required to reestablish a null at prescribed solenoid currents. The effective Verdet constant was found to be compatible with handbook values for crown glass at $\lambda=6328$ Å: $V\sim 2\times 10^{-2}$ arc min/Oe. The Faraday cell tests therefore establish the actual sensitivity of the polarimeter.

In one set of performance measurements, the signal-to-noise ratio was measured as a function of integration time for a broad range of drive frequencies ($0.01-10^5$ Hz). In these measurements, a weak magneto-optic signal (a Faraday rotation of $\phi=9.2\times 10^{-6}$ rad) produced by a 100 mA solenoid current was used. This rotation is approximately equivalent to 1/3 of the Kerr rotation produced by a one-monolayer Fe film. In optical experiments where the noise is dominated by statistical fluctuations associated with the number of photons detected, the signal-to-noise ratio can be calculated from the detected flux, and should vary as $\sqrt{T}$ where T is the signal integration time. If the waveform is sampled N times per cycle, the accumulated dwell time per sample can be defined as $t_d=(T/N)$. The effective signal integration time in a system that utilizes an A/D conversion depends not only on the run time of a measurement, but also on an analog integration time constant τ.

Measurements of the signal-to-noise ratio plotted as a function of $\sqrt{\tau}$ over the appropriate range of parameters yielded the expected linear dependence, demonstrating that the analog averaging technique is effective.[18] Measurements of the signal-to-noise ratio plotted as a function of $\sqrt{t_d}$ also yielded linear dependence at higher drive frequencies f_d $>$few kHz, and for dwell times t_d that yielded signal-to-noise ratios below about 30. Longer integration times continued to improve the signal-to-noise ratio, but the experimental values departed from the theoretical predictions, an indication of the presence of nonstatistical noise sources. The departures of the measured signal-to-noise ratio from the theoretical limit based on statistical noise increased as the drive frequency was reduced. Figure 5 presents a three-dimensional histogram that characterizes the signal-to-noise measurements. Generally, for frequencies above 10 Hz, signal-to-noise ratios increase as $\sqrt{t_d}$, and only depart significantly from theoretically predicted values for integration times that yield signal-to-noise ratios above 30. Below 10 Hz frequencies, the signal-to-noise ratios depart significantly from values predicted based only on statistical noise. The low frequency ($<$10 Hz) scaling of the signal-to-noise ratio exhibits a strong flicker noise component $f^{-\alpha}$ where $\alpha\sim 1$. Significant improvement in the S/N at low frequencies has been achieved by replacing the 300 MHz preamplifiers by Stanford Research Systems SR-560 low noise amplifiers (with lower bandwidth), or by replacing the PM tube/300-MHz dc amplifiers with the silicon detector/integrated preamplifiers described earlier. The system can be upgraded to a two-channel 100 MS/s system by the addition of a second high-speed A/D card. With this upgrade, and the current spatial resolution of ~ 5 μm, the polarimeter can be used to measure domain wall velocities in a 5 μm structure as high as (approximately) 5 μm/10 ns (500 m/s).

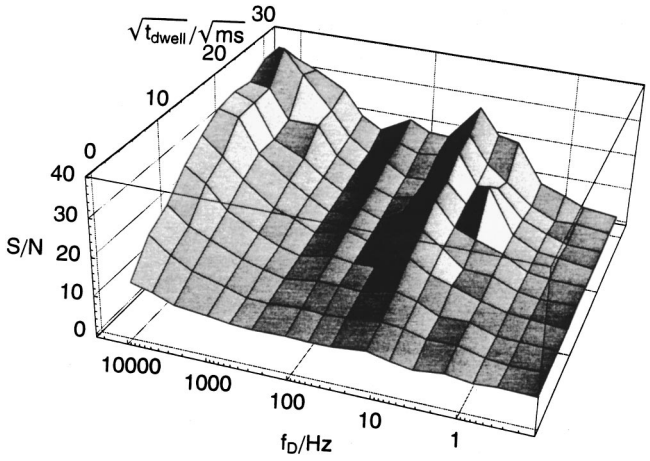

FIG. 5. Histogram of signal-to-noise ratio for polarimeter with 300 MHz preamplifiers. Z axis S/N ratio, *x* axis drive frequency (log scale), *y* axis square root of integrated dwell time (normalized to 1 ms).

ACKNOWLEDGMENTS

The authors wish to thank Joe Ting for designing and constructing the differential amplifier and Carlos Gutierrez (Southwest Texas State) for the Permalloy thin film sample. This work was supported by the National Science Foundation Grant Nos. DMR 9623494 and DMR 9704222. Marcus Heidkamp was supported in part by the DAAD through a student exchange program of the University of Würzburg, Germany.

[1] C. A. Ballentine, R. L. Fink, J. Araya-Pochet, and J. L. Erskine, Appl. Phys. A: Solids Surf. **49**, 459 (1989).
[2] S. D. Bader and J. L. Erskine, *Ultrathin Magnetic Structures II*, edited by

B. Heinrich and J. A. C. Bland (Springer, Berlin, 1994), p. 294.
[3] F. Schmidt, W. Rave, and A. Hubert, IEEE Trans. Magn. **21**, 1596 (1985).
[4] W. Rave, R. Schäfer, and A. Hubert, J. Magn. Magn. Mater. **65**, 7 (1987).
[5] R. Schäfer, J. Magn. Magn. Mater. **148**, 226 (1995).
[6] J. Giergiel and J. Kirschner, Rev. Sci. Instrum. **67**, 2937 (1996).
[7] H.-P. D. Shieh and M. H. Kryder, IEEE Trans. Magn. **24**, 2464 (1988).
[8] J. McCord, H. Brendel, A. Hubert, and S. S. P. Parkin, J. Magn. Magn. Mater. **148**, 244 (1995).
[9] S. Gadetsky, J. K. Erwin, and M. Mansuripur, J. Appl. Phys. **79**, 5687 (1996).
[10] R. P. Cowburn, D. A. Koltsov, A. O. Adeyeye, and M. E. Welland, Appl. Phys. Lett. **73**, 3947 (1988).
[11] M. R. Freeman, M. J. Brady, and J. Smyth, Appl. Phys. Lett. **60**, 2555 (1992).
[12] M. R. Freeman, W. K. Hiebert, and A. Stankiewicz, J. Appl. Phys. **83**, 6217 (1998).
[13] M. D. Schultz, T. Xue, and M. H. Kryder, J. Appl. Phys. **73**, 5776 (1993).
[14] P. Fumagalli, A. Rosenberger, G. Eggers, A. Münnemann, N. Heid, and G. Guntherodt, Appl. Phys. Lett. **72**, 2803 (1998).
[15] J.-S. Suen and J. L. Erskine, Phys. Rev. Lett. **78**, 3567 (1997).
[16] J.-S. Suen, M. H. Lee, G. Teeter, and J. L. Erskine, Phys. Rev. B **59**, 4249 (1999).
[17] D. Beaglehole, Rev. Sci. Instrum. **59**, 2557 (1988).
[18] Marcus Heidkamp, M. A. thesis, The University of Texas at Austin, 1998.
[19] The permalloy film was provided by Carlos Gutierrez at Southwest Texas State University.